Current Topics in The Physics of Fluids, 1 (1994)

Particle motion in rotating viscous fluids: Historical survey and recent developments

J.W. M. Bush*, H.A. Stone[1] and J.P. Tanzosh[1]

*Department of Applied Mathematics & Theoretical Physics, University of Cambridge, Cambridge CB3 9EW, England, [1]Division of Applied Sciences, Harvard University, Cambridge, MA 02138, USA

Abstract

A comprehensive survey of particle motion in rotating fluids is presented. Particle motion in directions both parallel and perpendicular to the axis of rotation and in both bounded and unbounded geometries is described. Various theoretical and experimental investigations are summarized in tabular form, as are the associated results deduced for the hydrodynamic force on the particle. Descriptions of the flows induced by the particle motion are also presented.

1. Introduction

The motion of an isolated body leaves us with a feeling of understanding when we can visualize the forces on the body, and so imagine how the body will move in accordance with Newton's laws. In high viscosity fluids, for example, the body forces acting on a steadily translating particle are balanced by a retarding frictional force. In rapidly rotating flows, however, the fluid motions induced by particle motion are more complex, as are the associated hydrodynamic forces acting on the particle. In particular, the anisotropy imposed by a fluid's solid body rotation ensures that the components of the hydrodynamic force in directions parallel and perpendicular to the rotation axis be entirely different.

Proudman [1] and Taylor [2] predicted theoretically that a particle translating slowly through a rapidly rotating low viscosity homogeneous fluid will be accompanied by a column of fluid circumscribing the particle and aligned with the rotation axis. The early experiments of Taylor [3-5] confirmed this "blocking" phenomenon and the existence of the so-called "Taylor column" structures. An example of the Taylor column structure accompanying the rise of a buoyant drop is provided in Figure 1. Many theoretical and experimental studies have since examined the influence of viscous and inertial effects on the structure of Taylor columns accompanying particle motion, and on the hydrodynamic force effecting the particle. The problem of particle motion through viscous rotating fluids has received considerable attention due to its importance in a variety of industrial applications.

The motion of rigid particles or drops in rotating fluids occurs in a variety of industrial applications of centrifugation; for example, the manufacturing of monodisperse latex microspheres [6], hollow shells [7], the inference of molecular weights [8], the thermocapillary fining of glass melts [9], electrophoresis of gas bubbles [10], the separation of valuable minerals (e.g. uranium), extraction of proteins and other macromolecules in biological and pharmaceutical operations, and industrial and municipal waste treatment [11,12]. In addressing a number of these problems, investigators often apply theory from the viscously dominated flow limit even when it is not warranted [13].

Rotationally-induced blocking effects may also be significant in a number of geophysical and planetary flows. While rotation dominates the large-scale dynamics of planetary atmospheres and oceans, the

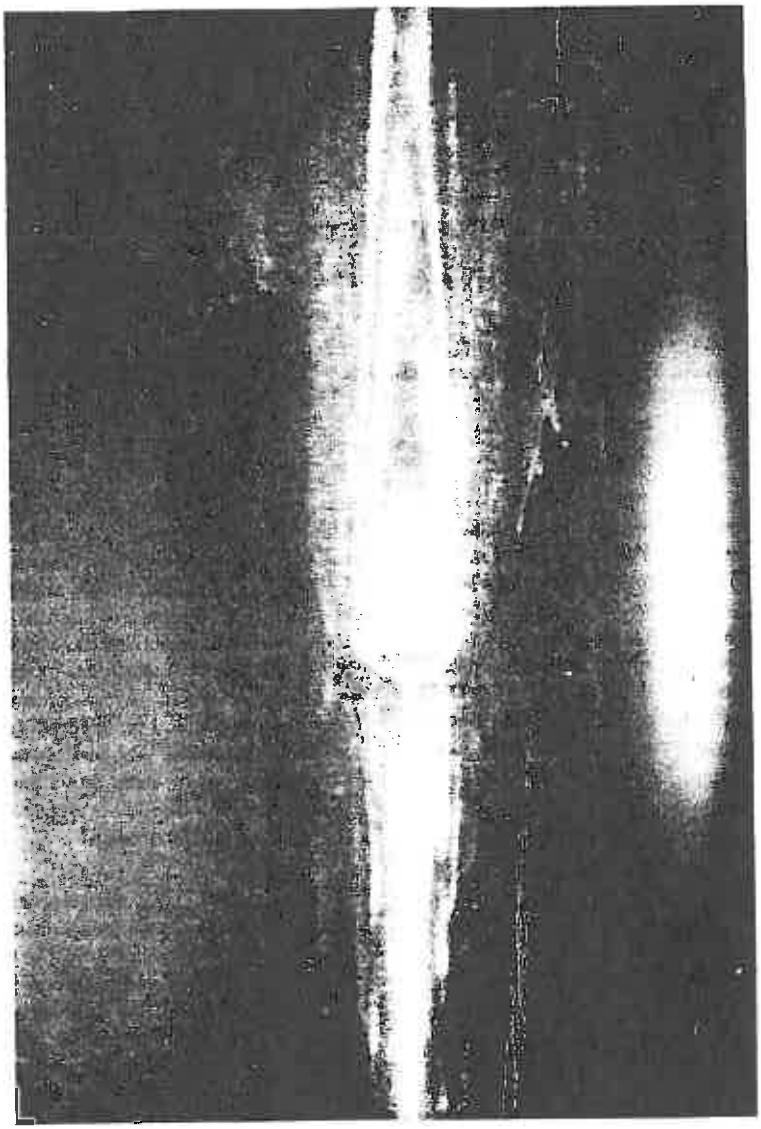

Figure 1: A drop of silicone fluid of radius 0.5 cm rising through a tank of water rotating at 56 rpm. This configuration corresponds to the effectively unbounded geometry (see Section 3). A Taylor column flow structure is clearly evident.

effects of stratification and fluid inertia generally tend to suppress Taylor column formation in flow past surface or seafloor topographic features. Nonetheless, regions of blocked fluid have been observed above seamounts in the oceans (e.g. [14]), and the interaction of bottom topography, rotation and stratification is a problem of great interest in geophysical fluid dynamics (for a review, see [15]). Hide [16] suggested that Jupiter's Great Red Spot may be the surface manifestation of a Taylor column extending above an obstacle at the bottom of the Jovian atmosphere. This theory has been criticized by Stone & Baker [17], and alternative explanations have been proposed [18]. It has also been recently suggested that Taylor column phenomena may influence motions within the Earth's liquid outer core, whose degree of stratification is very poorly known. In particular, Moffatt [19] proposed a model of core convection characterized by discrete parcels of buoyant fluid rising under the influence of the Earth's rotation with accompanying Taylor columns.

We here review a number of theoretical and experimental investigations of particle motion in rotating fluids. We consider independently motions parallel and perpendicular to the rotation axis, and henceforth refer to these motions as, respectively, 'axial' and 'transverse'. The effects of container boundaries in both problems are considered. We also describe the effects of particle shape on the dynamics, as well as the extension of a number of the rigid particle results to the case of a deformable fluid drop. In addition to summarizing the various results for the hydrodynamic force on the particles, we illustrate, wherever possible, the form of the fluid motion induced. In particular, we summarize criteria for Taylor column formation for both axial and transverse particle motion.

In Section 2, we present the equations governing both particle and fluid motion in a rotating system. The inviscid and viscously dominated flow limits are discussed and a brief review of Ekman boundary layers and the transient spin-up process is provided. In Section 3, we consider the case of axial particle motion and consider separately both unbounded and bounded flow geometries. The case of transverse particle motion is treated in Section 4. The relation between the dynamics of isolated particles and rotating suspensions is discussed in Section 5. In Section 6, we briefly describe two related problems in which a strong two-dimensional constraint is imposed on the fluid motion; namely, particle motion through electrically conducting fluids in the presence of a strong magnetic field, and particle motion through stratified fluids.

2. Governing Equations

2.1 Force Balance on the Particle

Consider a fluid domain of uniform density ρ and kinematic viscosity ν rotating with constant angular velocity $\mathbf{\Omega}$ in a uniform gravity field $\mathbf{g}$. We introduce a cylindrical coordinate system (r, θ, z) with origin on the axis of rotation and with the z-axis vertical, so that $\mathbf{\Omega} = \Omega\,\hat{\mathbf{z}}$ and $\mathbf{g} = -g\,\hat{\mathbf{z}}$. A particle of mass m and density $\rho - \Delta\rho$ located a distance r off-axis and translating with velocity $\mathbf{U}$ is subject to Coriolis, centrifugal and gravitational body forces, respectively, $-2m\mathbf{\Omega} \wedge \mathbf{U}$, $mr\Omega^2\hat{\mathbf{r}}$ and $-mg\hat{\mathbf{z}}$ (refer to Figure 2). The particle is also subject to a force associated with hydrostatic and centrifugal pressure gradients within the fluid given by $-m'r\Omega^2\hat{\mathbf{r}}+m'g\hat{\mathbf{z}}$, where $m' = \rho V$ is the mass of the liquid displaced by a particle with volume V. In addition, the particle experiences a hydrodynamic force $\mathbf{F}_h$ associated with its motion relative to the liquid. We thus write the force balance on the particle (written relative to the rotating frame) as

$$m\frac{d\mathbf{U}}{dt} = \mathbf{F}_h - \Delta\rho\, V\, \mathbf{g} - 2\,m\,\mathbf{\Omega}\wedge\mathbf{U} - \Delta\rho\, V\,\Omega^2\, r\,\hat{\mathbf{r}}\,, \tag{2.1}$$

where the hydrodynamic force on the particle is given by integrating the dynamic stresses over the particle surface S,

$$\mathbf{F}_h = -\int_S p_d\,\mathbf{n}\,dS + \int_S \mathbf{n}\cdot\boldsymbol{\tau}\,dS\,. \tag{2.2}$$

Here $\boldsymbol{\tau}$ is the deviatoric stress tensor, and the dynamic pressure p_d is related to the fluid pressure p by subtracting the hydrostatic and centrifugal pressure components:

$$p_d = p + \rho\,g\,z - \frac{\rho}{2}\,\Omega^2\,r^2\,. \tag{2.3}$$

In general, the force balance equation (2.1) must be accompanied by a torque balance equation relating

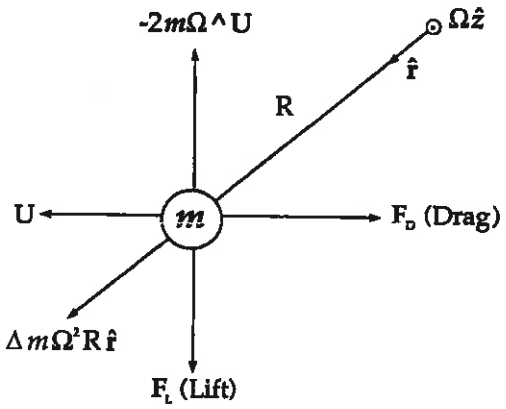

Figure 2: Forces acting on a particle translating in a plane perpendicular to the rotation axis include the Coriolis force, the centrifugal force, and the hydrodynamic force, which is decomposed into its drag and lift components. $\Delta m = m - m'$ is the difference between the mass of the particle and the displaced fluid.

the particle's rate of change of angular velocity to the applied and hydrodynamic torques. Imparting spin to a particle will influence the flow around the particle and so also the hydrodynamic force on the particle: the conservation of linear and angular momentum of the particle thus couple through the fluid equations of motion.

When a particle translates steadily in an axial direction, equation (2.1) indicates a balance between the buoyancy and hydrodynamic forces. When the particle translates in a plane perpendicular to the rotation axis, the hydrodynamic force may be decomposed into two components: the drag force, which acts to oppose the particle motion, and the 'lift' force, which acts perpendicular to U and Ω (refer to Figure 2). A solution for the hydrodynamic force on the particle requires detailed knowledge of the form of the flow around the particle and the associated pressure and viscous stress distributions over the particle surface. In general, the magnitude of the axial, drag and lift forces depends critically on the parameter regime describing the external flow.

2.2 Fluid Equations of Motion

In a frame rotating uniformly with angular velocity $\mathbf{\Omega}$, the fluid velocity $\mathbf{v}(\mathbf{r}) = (u, v, w)$ is related to that in the stationary frame, $\mathbf{u}(\mathbf{r})$, by $\mathbf{v}(\mathbf{r}) = \mathbf{u}(\mathbf{r}) - \mathbf{\Omega} \wedge \mathbf{r}$, and the Navier-Stokes equations for an incompressible flow take the form [20]

$$\frac{\partial \mathbf{v}}{\partial t} + \mathbf{v}\cdot\nabla\mathbf{v} + 2\,\mathbf{\Omega}\wedge\mathbf{v} = -\frac{1}{\rho}\nabla p_d + \nu\,\nabla^2\mathbf{v}\,, \qquad \nabla\cdot\mathbf{v} = 0\,. \tag{2.4}$$

In early theoretical studies of particle motion in rotating fluids, inertial effects were introduced through considering the unsteady inviscid equations [21]:

$$\rho\left(\frac{\partial \mathbf{v}}{\partial t} + 2\,\mathbf{\Omega}\wedge\mathbf{v}\right) = -\nabla p_d \quad , \quad \nabla\cdot\mathbf{v} = 0\,. \tag{2.5}$$

Stewartson [22-25] considered the time-dependent problems of an impulsively started rigid body translating in directions both parallel and perpendicular to the rotation axis through an inviscid fluid, and thus deduced the steady asymptotic behaviour of the flow and the hydrodynamic force on the particle at long times. It is noteworthy that in these particular problems the ultimate state of the *transient inviscid* problem corresponds to the solution of the *steady viscous* equations (2.6) [20]. This correspondence is not generally valid, but appears to depend on the particle shape [26]. Since these early studies, solutions have primarily been sought to the steady viscous equations of motion in which all inertial terms are neglected (see, for example, Tables 1-5).

When focussing on the effects of fluid viscosity on particle motion in rotating fluids, it is convenient to choose length, velocity, time, and pressure scales of, respectively, a (a characteristic particle dimension), U, a/U, and $\mu U/a$, so that the dimensionless momentum equation assumes the form

$$\mathcal{R}_e\left(\frac{\partial \mathbf{v}}{\partial t} + \mathbf{v}\cdot\nabla\mathbf{v}\right) + 2\mathcal{T}\;\hat{\mathbf{z}}\wedge\mathbf{v} = -\nabla p_d + \nabla^2\mathbf{v}\,. \tag{2.6}$$

The Reynolds number, $\mathcal{R}_e = Ua/\nu$, characterizes the relative importance of inertial and viscous forces, while the Taylor number, $\mathcal{T} = \Omega a^2/\nu$, that of Cori-

olis and viscous forces. Alternatively, the flow may be characterized by the Rossby number, $\mathcal{R}_o = U/\Omega a = \mathcal{T}^{-1}\mathcal{R}_e$, which characterizes the relative importance of inertial and Coriolis forces, and the Ekman number, $\mathcal{E}_k = \mathcal{T}^{-1}$, which characterizes that of viscous and Coriolis forces.

The majority of research on particle motion in rotating flows has been concerned with the low Reynolds number limit where local and convective acceleration effects are negligible. In this case, particle motion is described completely in terms of the Taylor number $\mathcal{T}$:

$$2\mathcal{T}\hat{\mathbf{z}}\wedge\mathbf{v} = -\nabla p_d + \nabla^2\mathbf{v} \quad , \quad \nabla\cdot\mathbf{v} = 0 \, . \tag{2.7}$$

Most theoretical research has investigated the translation of isolated rigid particles along or perpendicular to the rotation axis in the asymptotic limits of either small or large Taylor numbers.

2.3 The Viscous Limit ($\mathcal{T} \ll 1$)

In many problems involving centrifugal separation, the Reynolds and Taylor numbers are small; consequently, the flow induced by the centrifugally-forced particle motion is typically treated as a Stokes flow: the hydrodynamic force on the particle corresponds precisely to the Stokes drag $-6\pi\mu a\mathbf{U}$, and the lift force vanishes. Particle trajectories for the centrifugally and gravitationally forced motion of a rigid sphere [6] and a spherical bubble [27] in a Stokes flow have been deduced. Experimental investigations of particle motion at small but non-zero $\mathcal{T}$ [7,28] indicate that slight corrections to the Stokes drag coefficients are required in order to match observed particle trajectories. For example, Moll [29] argued that the anomalously low efficiency of commercial centrifuges used to clean sewage was related to enhanced drag on the particles associated with the presence of Taylor columns.

In the limit where viscous effects dominate, rotation makes a small correction to the Stokes drag on a particle. The first theoretical study of the low $\mathcal{T}$ limit was presented by Childress [30] for the motion of a rigid sphere along the rotation axis and the corresponding motion perpendicular to the rotation axis was described by Herron et al. [31]. In both these cases the correction to the Stokes drag is $O(\mathcal{T}^{1/2})$, as is the lift force introduced in the transverse problem (see equation 4.1).

2.4 The Geostrophic Limit ($\mathcal{T} \gg 1$)

For a sufficiently slow-moving and low-viscosity fluid, inertial and viscous effects may be ignored within the bulk of the fluid, where a 'geostrophic balance' exists between Coriolis and pressure forces:

$$2\,\hat{\mathbf{z}}\wedge\mathbf{v} = -\nabla p_d \, , \tag{2.8}$$

where p_d has been rescaled with a characteristic geostrophic pressure $\rho U\Omega a$. Taking the curl of equation (2.8) yields the Taylor-Proudman constraint of two dimensionality:

$$\frac{\partial\mathbf{v}}{\partial z} = \mathbf{0}. \tag{2.9}$$

The Taylor-Proudman theorem requires that all fluid motions in a geostrophically balanced incompressible flow be independent of the spatial coordinate that varies in a direction parallel to the axis of rotation. Consequently, when a rigid axisymmetric body translates slowly through a low viscosity fluid rotating rapidly about a vertical axis, a vertical column of fluid accompanies the body.

When the bulk flow is geostrophic, viscous effects are confined to thin boundary layers. While such boundary layers generally occupy only a small fraction of the fluid domain, they often play an important role in establishing weak secondary circulations within the geostrophic bulk. For example, as will be discussed in Section 3, a buoyant particle in a rapidly rotating bounded plane layer of fluid rises only by virtue of boundary layer transport over the particle and container surfaces. A brief discussion of boundary layer transport in rotating fluids, its importance in the spin-up process, and its interpretation in terms of vorticity dynamics is presented in the next three subsections.

EKMAN LAYERS AND EKMAN COMPATIBILITY: A simple yet illustrative example of a viscous boundary layer in the high $\mathcal{T}$ limit is the classical Ekman spiral solution which arises when a geostrophic swirling motion (e.g. $\mathbf{v} = V(r)\hat{\theta}$) is disrupted by a rigid horizontal boundary. The viscous boundary layer (or Ekman layer) has a characteristic thickness δ, which is necessarily small relative to the

particle dimension a: $\delta/a = \mathcal{T}^{-\frac{1}{2}} \ll 1$. Within the geostrophic exterior flow, the radial pressure force is balanced precisely by the Coriolis force associated with the swirling motion. Within the boundary layer, viscosity disrupts the swirling motion; consequently, the pressure gradient imposed on the boundary layer by the geostrophic exterior drives radial flow. The boundary layer flow assumes the Ekman spiral solution (e.g. [32]), which serves to match the geostrophic exterior to the rigid boundary.

Integrating the continuity equation across the boundary layer reveals that radial gradients in radial boundary layer fluxes require a vertical flow $w(r)$ into the boundary layer of magnitude

$$w(r) = \frac{\delta}{2r}\frac{\partial}{\partial r}\left(r\, v(r)\right) . \qquad (2.10)$$

This *Ekman compatibility* condition relates the magnitude of the primary geostrophic swirling motion $v(r)$ to that of the relatively weak, $O(\mathcal{T}^{-1/2})$, vertical flux into or out of the boundary layer. This viscously induced vertical flow is referred to as Ekman suction or pumping according to whether the flow is into or out of the boundary layer. Equivalent Ekman compatibility conditions may be derived for an axisymmetric interface between two immiscible geostrophically balanced flows [33-35].

SPIN-UP: An important paradigm in rotating fluid dynamics is the spin-up problem [20]. Consider a rigid cylindrical fluid-filled container of depth h and radius R (with $h = O(R)$) which rotates at an angular speed Ω about the cylinder's symmetry axis. The fluid is initially at rest relative to the container. At some time $t = 0$ the rotation rate of the container increases to $\Omega(1+\epsilon)$. Ekman layers are established on the top and bottom container boundaries on a rotational timescale, and serve to transport fluid radially outwards within the boundary layer. Ekman suction draws fluid into the upper and lower boundaries and so drives a large-scale circulation which transports high angular momentum fluid radially inwards within the bulk of the fluid. The circulation is completed by vertical transport in viscous boundary layers on the side walls of the container.

As a ring of fluid of radius r and mass m contracts in the inviscid geostrophic interior, conservation of angular momentum mrv requires that the ring's angular speed v/r increase from Ω to $\Omega(1+\epsilon)$ as its radius decreases by an amount $\epsilon r/2$. Since the internal circulation is driven by the Ekman suction, which is characterized by a typical speed of $\mathcal{T}^{-1/2}\epsilon\Omega r$ at a radius r, the convective timescale is $O(\mathcal{T}^{1/2}/\Omega)$. This 'spin-up time' is $O(\mathcal{T}^{-1/2})$ *smaller* than the timescale of diffusive adjustment, h^2/ν. In the absence of the spin-down process (the reverse of the spin-up process), a cup of tea would take approximately half an hour to come to rest after stirring, and the tea leaves would not be swept towards the center of the cup by Ekman layer transport on the lower boundary.

VORTICITY DYNAMICS: A number of important features of rotating flows may be most simply understood in terms of vorticity dynamics. Taking the curl of (2.4) yields an equation governing the evolution of the relative vorticity, $\omega = \nabla \wedge \mathbf{v}$, of the fluid,

$$\frac{\partial \boldsymbol{\omega}}{\partial t} + \mathbf{v}\cdot\nabla\boldsymbol{\omega} = (2\,\boldsymbol{\Omega} + \boldsymbol{\omega})\cdot\nabla\mathbf{v} + \nu\,\nabla^2\boldsymbol{\omega} . \quad (2.11)$$

In an Ekman layer, a steady state is established by a balance between diffusion of vertical vorticity across the boundary layer and the vortex compression or stretching associated with the vertical velocity gradient across the layer,

$$2\,\Omega\,\frac{\partial w}{\partial z} \approx \nu\,\frac{\partial^2 \omega_z}{\partial z^2} . \qquad (2.12)$$

One may thus alternatively view the spin-up process as being associated with the stretching of the basic state vorticity by the Ekman suction into the upper and lower boundary layers. Within the inviscid geostrophic interior, the vorticity evolves according to

$$\frac{\partial \boldsymbol{\omega}}{\partial t} = 2\,\boldsymbol{\Omega}\cdot\nabla\mathbf{v} , \qquad (2.13)$$

from which scaling confirms that the fluid's vertical vorticity will increase by an amount $\epsilon\Omega$ through vortex stretching (by the vertical velocity gradient $w/h = \epsilon\Omega\mathcal{T}^{-1/2}$) after a spin-up time.

3 Axial Particle Motion

3.1 Criteria for Taylor Column Formation

In order for a columnar structure to accompany a rigid sphere translating axially with speed U, Taylor [4] observed that the Rossby number $\mathcal{R}_o = U/\Omega a$ based on the sphere radius a must be less than a critical value equal approximately to $1/\pi$. The experiments of Long [36] imply a similar critical Rossby number of 0.2. Analytical studies of axial particle motion at finite Rossby number have been performed by Stewartson [37], Lighthill [38] and Greenspan [20]. Stewartson deduced a solution for inviscid flow past an axisymmetric body on the basis of Oseen's equations, and inferred a critical Rossby number of 0.348. Lighthill explained the Taylor blocking phenomenon in terms of the propagation of inertial waves from the body, and so concluded that the body should have a forward influence on the flow at all Rossby numbers. On the basis of the solution for the axial motion of a rigid disc started impulsively in an inviscid flow, Greenspan concluded that substantial Taylor blocking would occur for $\mathcal{R}_o < 0.675$. The experiments of Pritchard [39] suggest that there is weak blocking at all Rossby numbers, and that substantial Taylor column formation occurs for $\mathcal{R}_o < 0.7$.

In the case of particle motion at negligibly small Rossby number, the Taylor column which circumscribes a body rising on-axis has a vertical extent determined by the fluid viscosity ν. In particular, theory predicts that a truncated Taylor column, or "Taylor slug", will extend a characteristic distance $a\mathcal{T}$ up- and downstream of a sphere of radius a [40] (see the scaling argument presented in Section 3.2). Maxworthy's [41] experiments revealed Taylor columns to be typically an order of magnitude shorter. Similarly, the numerical results of Tanzosh & Stone [42] for a sphere translating axially at $\mathcal{R}_o = 0$ indicate a blocked region of length $0.116a\mathcal{T}$ at large Taylor numbers (refer to Figure 3; see also [43]). The problem of axial particle motion in rotating fluids will be subdivided according to whether the Taylor column accompanying the particle interacts with the container boundaries.

3.2 Unbounded Geometry

Table 1 summarizes theoretical studies of axial particle motion through unbounded rotating fluids. Various analytical and experimental deductions of the hydrodynamic drag on the particle are presented in Table 2. The hydrodynamic drag on a rigid sphere varies dramatically according to the magnitudes of the nondimensional groups characterizing the particle motion.

Morrison & Morgan [44] considered the steady

$\mathcal{T}$	shape	method	reference
0	sphere	exact solution	e.g. Batchelor [32]
$\ll 1$, ($\mathcal{R}_e/\sqrt{\mathcal{T}}$ fixed)	sphere	matched asymptotic expansion	Childress [30]
$\gg 1$	disc/sphere	unsteady, inviscid analysis	Stewartson [22]
"	"	boundary layer analysis	Morrison & Morgan [44]
"	"	"	Moore & Saffman [40]
"	bubble/drop	"	Bush et al. [48]
arbitrary	sphere	multipole expansion	Weisenborn [45]
arbitrary	disc	dual integral equations	Vedensky & Ungarish [43]
arbitrary	sphere/ellipsoid	boundary integral equation	Tanzosh & Stone [42]
< 1	sphere	numerical: finite difference, series expansion ($\mathcal{R}_e < 1$)	Dennis et al. (1982)

Table 1: Theoretical studies of particle motion along the axis of an unbounded rotating fluid.

$\mathcal{R}_e$	$\mathcal{T}$	$\mathcal{R}_o$	Drag	Reference
0	NA	NA	$6\,\pi\,\mu\,a\,U$	e.g. Batchelor [32]
0	$\ll 1$	0	$6\pi\mu aU\left(1+\frac{4}{7}\,\mathcal{T}^{1/2}\right)$	Childress [30]
0	$\ll 1$	0	$6\pi\mu aU\left(1+\frac{4}{7}\,\mathcal{T}^{1/2}+\frac{16}{49}\,\mathcal{T}\right)$	Weisenborn [45]
NA	$\gg 1$	0	$\frac{16}{3}\,\rho\,a^3\,\Omega\,U$	Stewartson [22]
0	$\gg 1$	0	$\frac{16}{3}\,\rho\,a^3\,\Omega\,U$	Moore & Saffman [40]
NA	$\gg 1$	$\ll 1$	$2.6\,\pi\,\rho\,a^3\,\Omega\,U$	Maxworthy [41]
NA	$\gg 1$	$0.5-1.4$	$8.2\,\pi\,\rho\,\Omega^2\,a^4$	Maxworthy [41]
NA	$\gg 1$	$\gg 1$	$\frac{\pi}{10}\rho a^2U^2(\frac{7}{2}-\frac{4}{\mathcal{R}_o^{1/2}}\ln\frac{2}{\mathcal{R}_o}-\frac{12}{\mathcal{R}_o^{1/2}})$	Stewartson (1968)
$\gg 1$	NA	$\gg 1$	$\frac{\pi}{2}\,\rho\,a^2\,U^2$	Schlichting (1979)

Table 2: Analytical approximations to the hydrodynamic drag on a rigid sphere of radius a translating on-axis with velocity U through an unbounded fluid rotating about a vertical axis with angular velocity Ω. The symbol NA denotes 'not applicable'. The results of Maxworthy are based on experiments.

motion of a rigid disc in an unbounded viscous fluid for $\mathcal{T} \gg 1$. This problem was generalized by Moore & Saffman [40] to the case of an arbitrarily-shaped rigid axisymmetric particle with equatorial radius R. For this high $\mathcal{T}$ limit, radial velocity gradients occur on a particle lengthscale R, while axial gradients occur on a scale corresponding to the length of the Taylor column $L \gg R$. The pressure difference up- and downstream of the particle is associated with the geostrophic swirling motions of opposite sense above and below the particle, and so is approximately given by $\Delta P \approx \rho\Omega v R$, where v is a typical swirl velocity. From continuity, radial velocities u are smaller than axial velocities w according to $u \approx wR/L$. The dominant balance in the azimuthal component of (2.7) is $\Omega u \approx \nu v/R^2$, and so indicates that $v \approx \mathcal{T}u$. Similarly, the axial component yields $\Delta P/L \approx \nu\rho w/R^2$. Combining these estimates indicates that the Taylor column assumes a length $L \approx R\mathcal{T}$, and that the swirling motions generated are comparable in magnitude to the particle's rise speed: $v \approx U$. Balancing the geostrophic pressure drag $\pi R^2\rho\Omega UR$ with the buoyancy force $g\Delta\rho V$ yields an estimate for the steady rise speed: $O(\rho R^3\Omega U)$. For a sphere of radius a the exact result is listed in Table 2.

Figure 3 illustrates schematically the form of the flow at moderate Taylor numbers ($\mathcal{T} > 50$) induced by a particle rising on-axis, and subdivides the flow into five distinct regions: the Ekman layer on the particle surface; the geostrophic regime (in which swirling motions of characteristic magnitude U and of opposite sense arise above and below the drop); the recirculating region (which bears some resemblance to the wake associated with a particle translating through a nonrotating fluid at moderate Reynolds numbers); the Stewartson layer, a viscous internal boundary layer region which transports fluid vertically around the particle; and the

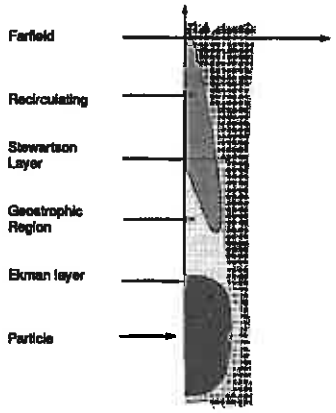

Figure 3: Regions in the flow field of a particle translating along the axis of a fluid in solid-body rotation when $\mathcal{T} > 50$: Ekman layer, geostrophic region, recirculating region, far field, Stewartson layer. (The horizontal and vertical scales are distorted.)

unperturbed far-field. Figure 4 illustrates the numerically determined extent of several of these regions as a function of the Taylor number [42]. The two-dimensional constraint imposed by the fluid's rotation is released through viscous effects, which permit large-scale streaming past the body in the Stewartson layers. Finally, Figure 5 illustrates the dependence of drag on a rigid sphere as a function of $\mathcal{T}$, and indicates that the low $\mathcal{T}$ result of Childress [30], when augmented by the high $\mathcal{T}$ result of Stewartson [22], provides a good approximation for the drag at all $\mathcal{T}$ [42,45].

In the high $\mathcal{T}$ limit, the fluid transported through the Stewartson layers greatly exceeds that through the Ekman layers on the particle surface. Consequently, the hydrodynamic drag does not depend on the details of the boundary layer on the particle surface. In particular, the drag is independent of the detailed shape of the particle, and depends only on its equatorial (maximum) radius: a disc and sphere of equal buoyancy and radius will rise at identical speeds.

DEFORMABLE DROPS: Since the details of the boundary layer on a buoyant particle rising in an unbounded fluid in the high $\mathcal{T}$ limit are not important, the extension of the rigid particle problem to the case of a deformable fluid drop rising on-axis is straightforward [35]. As in the case of the rigid particle, the drop rise speed is determined by the drop's buoyancy and equatorial radius R. The rise speed of a deformable drop in an unbounded fluid is thus determined by the drop shape, which requires consideration of the normal stress balance at the drop interface. In the high Taylor number limit, geostrophic and hydrostatic pressures do not contribute significantly to the normal stress balance at the drop surface, which is dominated by centrifugal pressures and curvature forces associated with the drop's interfacial tension σ. The drop thus assumes the form of a prolate ellipsoid whose degree of distortion is prescribed by the rotational Bond number, $\Sigma = -\Delta\rho\Omega^2 R^3/8\sigma$, which indicates the relative importance of centrifugal and interfacial tension forces. The drop shapes correspond to those observed in spinning drop tensiometers in the absence of drop translation [35,46-48], and the shape and rise speed are uniquely prescribed by the single parameter Σ. In the limit of large surface tension, the drop assumes a spherical form and its rise speed (which, according to Table 2, scales as $1/R^3$) is a minimum. As rotational effects become more important, the drops become progressively more prolate, and the rise speed increases.

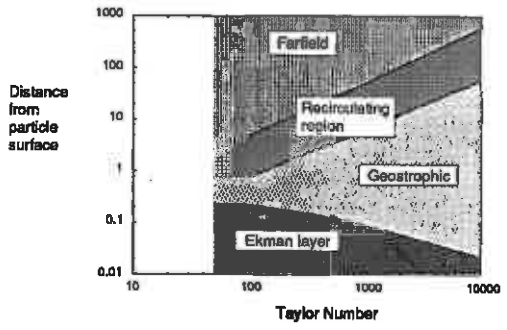

Figure 4: Distance from the particle surface $(z-1)$, measured along the centerline, of the boundaries between different regions of the flow. For sufficiently large Taylor number, the height of the Ekman layer scales as $2.5\mathcal{T}^{-1/2}$, the geostrophic region as $0.006\mathcal{T}$ and the recirculating region as $0.052\mathcal{T}$. [42]

3.3 Bounded Geometry

If a buoyant particle rises through a sufficiently shallow horizontal fluid layer, the Taylor column accompanying the particle will span the entire fluid depth: the body cannot rise unless the Taylor-Proudman constraint is released. The problem of bounded particle translation was first treated by Moore & Saffman [49], who considered the rise of rigid axisymmetric bodies at high $\mathcal{T}$. This work was extended to the case of a deformable bubble rising along the rotation axis by Bush et al. [48], who also generalized the results to the case of a deformable drop of arbitrary viscosity [35]. The case of viscously truncated Taylor columns comparable to the length of the container was considered by Hocking et al. [50] (see also [51]).

In the high $\mathcal{T}$ limit, geostrophic flow arises in the bulk of the fluid and viscous effects are confined to thin Ekman layers on the container and particle boundaries, as well as the internal boundary layers

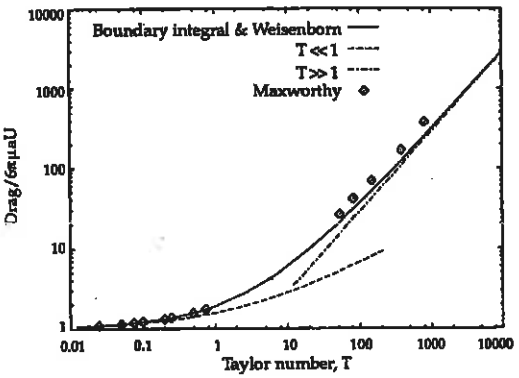

Figure 5: Drag on a rigid sphere versus Taylor number using: (i) the boundary integral method [38] and a multipole expansion [40] (solid curve); (ii) experimental results of Maxworthy [41,53] (symbols); (iii) matched asymptotic expansion for $\mathcal{T} \ll 1$ [30] (dashed curve); (iv) inviscid, unsteady, geostrophic analysis for $\mathcal{T} \gg 1$ [22] (dotted-dashed curve). The simple expression $|\mathbf{F}_H|/6\pi\mu aU = 1 + (4/7)\mathcal{T}^{1/2} + (8/9\pi)\mathcal{T}$, which combines the low and high Taylor number asymptotic limits, is within 5% of the numerical results for *all* Taylor numbers [42].

(Stewartson layers [49,52]) which define the vertical walls of the Taylor column. Vortex compression and stretching in, respectively, the regions up- and downstream of the particle give rise to geostrophic swirling motions of opposite sense above and below the particle. Ekman suction and pumping on, respectively, the upper and lower container and particle boundaries serve to transport fluid from the fore to the aft column regions. Continuity requires that there be a net down-flow in the Stewartson layers. Figure 6 illustrates schematically the form of the flow induced by a fluid drop bound by surface tension and rising along the length of a Taylor column in the case where both internal and external flows are geostrophic.

As demonstrated in the discussion of Ekman compatibility conditions (Section 2.4), $O(1)$ geostrophic swirling motions are associated with $O(\mathcal{T}^{-1/2})$ ageostrophic vertical motions. Consequently, we expect the geostrophic swirling motions to be $O(\mathcal{T}^{1/2})$ larger than the rise speed U. The geostrophic high and low pressures existing, respectively, above and below the particle thus have characteristic magnitudes $P_g = \rho\Omega RU\mathcal{T}^{1/2}$, and the associated geostrophic pressure drag on the particle has a typical magnitude of $P_g\pi R^2$. The steady rise speed is deduced by balancing the geostrophic drag with the buoyancy force, $g\Delta\rho V$, and so has a characteristic magnitude

$$U_0 = \frac{V}{\pi R^4}\,\frac{\Delta\rho}{\rho}\,\frac{g}{\Omega}\left(\frac{\nu}{\Omega}\right)^{1/2} \qquad (3.1)$$

Note that the rise speed increases with fluid viscosity and decreases with increasing rotation rate. This dependence underlines the role of viscosity in the bounded geometry which is to release the constraint of two-dimensionality imposed by the fluid rotation.

In the bounded geometry, buoyant particles are able to rise only by virtue of the finite fluid viscosity, which permits boundary layer transport from the fore to the aft Taylor column regions. Consequently, the hydrodynamic drag depends explicitly on the details of the boundary layer on the particle surface. For example, the rise speed of a fluid drop

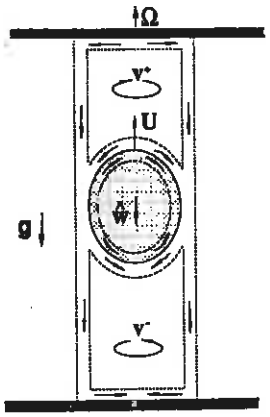

Figure 6: A schematic illustration of the flow induced by a low viscosity ('geostrophic') drop rising between rigid horizontal boundaries [35]. The drop interface is characterized by a double Ekman layer, and the internal flow by a weak downward flow.

depends not only on the its buoyancy and equatorial radius (as in the unbounded case), but also on its detailed shape and fluid properties [35]. In particular, the rise speed is now set by Σ and a viscosity ratio parameter $\beta = (\hat{\rho}/\rho)(\hat{\nu}/\nu)^{1/2}$ (where carats denote drop variables) which together prescribe the efficiency of the Ekman transport over the drop surface. Figure 7 illustrates the nature of the dependence of rise speed on Σ and β for the case of a drop rising between rigid boundaries. As in the unbounded case, the drop's rise speed increases as the drop becomes progressively more prolate and its equatorial radius decreases. Moreover, as β increases, the Ekman transport over the drop surface becomes progressively more efficient, and the rise speed increases. For example, the rise speed of a rigid sphere is larger by a factor of 105/43 than that of a bubble of equal size and buoyancy.

3.4 Arbitrary Taylor Numbers

Three recent papers have investigated axial particle motion at arbitrary values of the Taylor number. Vedensky & Ungarish [43] and Ungarish & Vedensky [51] present exact solutions for the axial rise speed of a rigid disc in, respectively, unbounded and bounded geometries. Hankel transform methods were used in order to arrive at a system of dual integral equations which was solved numerically. The solution allowed for a detailed examination of the evolution of the flow structure as the Taylor number was increased, and enabled the authors to identify the presence of the recirculating regions fore and aft of the particle. These studies have been complemented by Tanzosh & Stone's [42] general integral equation representation of the solution to equation (2.7). The integral equation must be solved numerically, but yields solutions for particles of arbitrary shape (a family of rigid ellipsoids was considered) translating axially at arbitrary Taylor numbers. Moreover, boundaries are, in principle, straightforward to incorporate with their solution method.

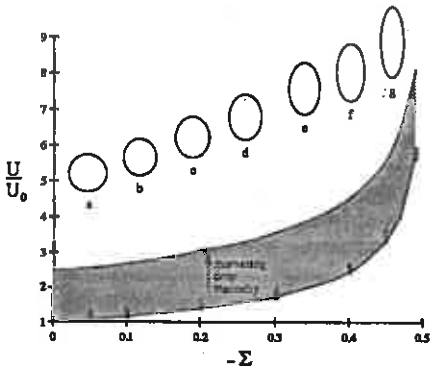

Figure 7: Rise speed and shape of a fluid drop bound by surface tension and rising on-axis between rigid horizontal boundaries, as a function of the rotational Bond number $\Sigma = -\Delta\rho\Omega^2 R^3/8\sigma$ [35]. The lower curve represents the rise speed of an inviscid drop and the upper curve that of an identically shaped rigid body. Rise speeds are normalized with respect to that of a spherical inviscid drop and deformed shapes are scaled such that the volumes correspond to that of the undeformed spherical drop.

3.5 Experiments

Taylor's early experiments [4] have motivated a number of experimental investigations of axial particle motion in rotating fluids, several of which have focussed on the effects of fluid inertia on the particle motion and so explored the dependence of rise speed and flow structure on $\mathcal{R}_o$ [36,39]. Only limited experimental work has been done in the low $\mathcal{R}_o$ limit, primarily due to the difficulties inherent in achieving this parameter regime in the laboratory. Maxworthy [53] investigated the dependence of rise speed on Taylor number in the low $\mathcal{T}$ and low $\mathcal{R}_o$ regime (see Figure 5) and so deduced the first effects of rotation on a sphere rising on-axis through a high viscosity fluid. Experimental investigations of rigid particle motion in the rapid rotation (high $\mathcal{T}$) limit have also been performed by Maxworthy in both the bounded [54] and effectively unbounded [41] geometries. Analogous studies of deformable drop motion have been performed by Bush et al. [35].

In an investigation of on-axis sphere motion in the bounded geometry, Maxworthy [54] demonstrated that the persistence of inertial effects in the laboratory results in steady rise speeds which are typically larger than those predicted theoretically by Moore & Saffman [49]. In particular, Maxworthy observed

that unless the inertial effects associated with the vigorous swirling motions within the Taylor column are negligible, weak radial flows develop within the Taylor column which serve to complement the Ekman boundary layers in transporting fluid from the fore to the aft Taylor column regions, releasing the Taylor-Proudman constraint of two-dimensionality and facilitating the rise of the drop. Similar difficulties were encountered in Bush et al.'s [35] experimental investigation of drop motion.

Maxworthy [41] also investigated particle motion in the unbounded flow geometry, and observed rise speeds which were typically a factor of $\pi/2$ smaller than those predicted theoretically by Stewartson [22] and Moore & Saffman [40]. This discrepancy was also observed in the drop experiments of Bush et al. [35]. Ungarish & Vedensky's recent theoretical work, as described in section 3.1.3, accounts for boundary effects at finite Taylor numbers and improves the comparison of the linear theory with Maxworthy's experimental results for long but finite containers. Nonetheless, there remain significant discrepancies between the unbounded theory and experimental observations [51].

4. Transverse Particle Motion

4.1 Criteria for Taylor Column Formation

According to the Taylor-Proudman theorem, when a spherical particle moves through a geostrophically balanced flow, the fluid inside the Taylor column circumscribing the sphere behaves as a rigid body, and the external fluid streams past as if the column were solid. As in the case of axial particle motion, however, the Taylor-Proudman constraint may be released through either viscous or inertial effects, so that this idealized picture of the flow is not easily realized.

Experiments reveal that in rapidly rotating fluids, transversely translating "fat bodies" tend to block fluid from entering a cylindrical region circumscribing the particle [5]. The Hide criterion [16] for Taylor column formation may be expressed as a requirement on the ratio of the vertical length of the particle h to the depth D of the fluid layer: $h/D > \mathcal{R}_o$, where the Rossby number is defined in terms of the object's width L: $\mathcal{R}_o = U/L\Omega$. Experiments [55,56] suggest that Taylor columns accompany transverse motion whenever $h/D > 0.5\ \mathcal{R}_o$, otherwise convective inertial effects preclude Taylor column formation.

The criteria for Taylor column formation for transverse particle motion in the zero Rossby number limit, in which the Taylor-Proudman constraint must be relaxed by viscous effects, is not well understood. Analytical [26] and recent numerical [57] studies suggest that "thin objects" such as a disc do not block the flow; however, there exists no equivalent of the Hide criterion for the transverse motion of fat bodies in the zero Rossby number limit.

4.2 Theory and Experiments

Tables 3 and 4 summarize, respectively, the analytical and experimental work related to transverse particle motion in rotating fluids. Table 5 summarizes a number of results for the hydrodynamic drag and lift forces on a sphere as deduced analytically or measured experimentally.

In addition to demonstrating the blocking phenomenon, Taylor [2] predicted theoretically and verified experimentally that when the flow around a body translating in the transverse direction is strictly two-dimensional, the hydrodynamic force on the body is equal and opposite to the Coriolis force on a mass of fluid with the same volume as the object. For example, Taylor observed that a vertical cylinder with the same density as the surrounding fluid translates through the fluid exactly as if the fluid were not rotating, as the Coriolis and lift forces on the cylinder precisely cancel. Conversely, when the flow about the body is three-dimensional, as was the case when Taylor dragged a neutrally buoyant sphere through the fluid, the Coriolis force exceeds the lift force; thus, if the tank is rotating in a counterclockwise sense, the body is deflected to its right.

Taylor's experiments were repeated by Hide & Ibbetson [55], who demonstrated the manner in which the Taylor-Proudman theorem was violated in the transverse motion of a sphere at small Rossby numbers. Deviations from the purely geostrophic motion included a weak flow across the Taylor column,

RESEARCHER	$\mathcal{R}_e/\mathcal{T}^{1/2}$	GEOMETRY	BOUNDARY	METHOD
$\mathcal{T} \ll 1$:				
Herron, Davis & Bretherton [31]	$\ll 1$	sphere	∞	matched asymptotic expansion
Davis (1992)	$O(1)$	sphere	∞	matched asymptotic expansion
Tanzosh & Stone [57]	$\ll 1$	disc	∞	dual integral equations
$\mathcal{T} \gg 1$:				
Stewartson [23]	$\ll 1$	$O(1)$	∞	unsteady, geostrophic
Jacobs [59]	$\ll 1$	$O(1)$	$O(1)$	boundary layer analysis
Stewartson [25]	$\ll 1$	$O(1)$	$O(1)$	unsteady, geostrophic
Moore & Saffman [40]	$\ll 1^a$	disc	[b]	boundary layer analysis
Ingersoll (1969)	$O(1)$	$O(\mathcal{R}_e/\mathcal{T})$; thin[c]	$O(\mathcal{T}/\mathcal{R}_e); \gg 1$	perturbation expansion
Vaziri & Boyer (1971)	$O(1)$	$O(\mathcal{T}^{-1/2})$; thin[c]	$O(\mathcal{T}); \gg 1$	numerical; finite difference

Table 3 : Analytical work related to the slow translation of a particle in a direction perpendicular to the rotation axis. The GEOMETRY refers to the particle height to width ratio and the BOUNDARY refers to the proximity of rigid boundaries. The ratio $\mathcal{R}_e/\mathcal{T}^{1/2}$ quantifies the importance of convective inertial effects in the flow. ([a]actually requires a less restrictive assumption $\mathcal{R}_o\,\mathcal{T}^{1/4} \ll 1$; [b]requires $H/D \ll \mathcal{T}^{1/2}$ so that Stewartson layers remain thin and also investigates the unbounded case; [c]assumes that the slope of the surface topology (particle) along the rotation direction is small).

RESEARCHER	$\mathcal{R}_e$	$\mathcal{R}_o$	$\mathcal{T}$	D/L	H/L	COMMENT
Taylor [5]						blocking
Hide & Ibbetson [55]	7–100	0.003–0.02	10^3–10^4	0.6	4.0	description; blocking/deflection
Hide & Ibbetson [56]			50–750			Taylor column bending; inertial effects
Vaziri & Boyer (1971)	120	0.04	3000	0.0625	5.0	shallow topography; deflection
Davies (1972)	25	0.01	2500	1	8	flow description
Mason [58]		0.001–1.0	25–250	1	3 – –20[a]	blocking/deflection; drag/lift
Maxworthy [61]		0.012	2150	400	5600	disc; streamline deflection
Karanfilian & Kotas [60]	0.03–3300	0.24–20	0.08–300	1	34	lift/drag

Table 4 : Experimental research related to the slow translation of a particle in a direction perpendicular to the rotation axis in finite containers. The columns delineate the approximate parameter range (Reynolds, Rossby and Taylor numbers) and geometry (H–tank depth; L–particle height, D–particle width). [a]indicates a free surface. Experiments in which Taylor blocking or streamline deflections were observed are indicated.

and a slightly altered external flow, both of which the authors concluded were viscous in origin. Mason [58] demonstrated that these ageostrophic effects vanish if the transverse motion is sufficiently slow, and so concluded that, had the Rossby number been sufficiently small in the experiments of Taylor, the neutrally buoyant sphere would have been undeflected by the Coriolis force.

Stewartson [23] examined the transverse translation of a rigid ellipsoid in an unbounded inviscid fluid through consideration of the unsteady geostrophic equations. As the length of the vertical axis of the ellipsoid increased from zero, the lift force in-

$\mathcal{R}_e$	$\mathcal{T}$	$\mathcal{R}_o$	Drag	Lift	Reference
0	∞	0	$6\pi\mu aU$	0	e.g. Batchelor [32]
≤ 0.5	< 1	$\ll 1$	$\approx 6\pi\mu aU$	≈ 0	Karanfilian & Kotas [60]
0	$\ll 1$	0	$6\pi\mu aU(1+\frac{3}{5}\mathcal{T}^{1/2})$	$\frac{3}{5}\ 6\pi\mu aU\ \mathcal{T}^{1/2}$	Herron et al. [31]
NA	∞	$\ll 1$	$0.98\ \rho V\Omega U$	$0.76\ \rho V\Omega U$	Stewartson [23]
NA	∞	$\ll 1$	0	$2\rho V\Omega U$	Stewartson [25]
NA	$\gg 1$	$\ll 1$	≈ 0	$2\rho V\Omega U$	Mason [58]
$\gg 1$	$\gg 1$	≈ 1	$\rho V\Omega U$	≈ 0	Mason [58]
$\gg 1$	$\gg 1$	$\gg 1$	$\frac{\pi}{2}\ \rho\ a^2\ U^2$	0	Mason [58]

Table 5: The hydrodynamic drag and lift forces on a rigid sphere of radius a and volume V translating in the plane perpendicular to the rotation axis $\hat{\mathbf{z}}$ with speed U. $2\rho V\Omega U$ is the Coriolis force which would act on an object with the same mass as the fluid displaced by the particle. The results of Mason [58] and Karanfilian & Kotas [60] are based on experiments. Mason's result for $\mathcal{R}_o \approx 1$ was found to be valid provided a Taylor column did not accompany the particle motion.

creased from zero to a value corresponding to the Coriolis force on a mass of fluid with the same volume as the object. Later, Stewartson [25] considered the transverse motion of a neutrally buoyant sphere between rigid horizontal boundaries, and deduced a solution for the hydrodynamic force in accord with that of Jacobs [59], whose solution was based on the steady viscous equations of motion. These solutions again indicate that the lift force exerted on a transversely translating particle at sufficiently small Rossby number is equal and opposite to the Coriolis force on the mass of fluid displaced by the particle. These conclusions have been verified in the experiments of Mason [58], who also observed that at very low Rossby numbers, the drag force experienced by a sphere is comparable in size to an order of magnitude estimate of the viscous forces. The critical Rossby number, below which a neutrally buoyant sphere was undeflected by the Coriolis force in a bounded plane layer, corresponds to that specified in the Hide criterion for Taylor column formation.

Mason also considered the case of moderate Rossby numbers, in which no Taylor columns were observed, and concluded that in this case both the drag and lift forces are comparable to but less than the Coriolis force on a mass of fluid with the same volume as the displaced fluid. Consequently, a neutrally buoyant sphere translating at moderate Rossby number through a tank of fluid rotating in a counterclockwise sense will be weakly deflected to its right, as was the case in Taylor's experiments. This moderate Rossby number regime was also examined by Karanfilian & Kotas [60], who investigated experimentally the free motion of a particle in a rotating fluid, and parameterized the drag and lift coefficients in various regions of parameter space. They concluded that in the limit of rapid rotation, the lift force has contributions from both the Coriolis force acting on the fluid surrounding the particle, and the induced spin of the particle relative to the liquid.

One problem where analytical progress has been possible on the viscous flow problem is for the case of transverse motion of a thin rigid disc in a plane perpendicular to the rotation axis. Moore & Saffman [26] investigated this problem in the high Taylor number limit for both bounded and unbounded geometries, and demonstrated that the disc motion was not accompanied by a Taylor column. Instead, fluid particles cross the regions above and below the particle and, in so doing, are deflected through a finite angle. For the case of a disc translating edgewise between rigid boundaries, Moore & Saffman [26] predict a streamline deflection of 18.4°, which is in remarkably good agreement with Maxworthy's [61] experimental measurement of 20°. Finally, Wilcox [62] considered the bounded transverse high $\mathcal{T}$ motion of a disc for the case where the disc is inclined relative to the horizontal boundaries.

Tanzosh & Stone [57] have recently presented an

exact solution for the translation of a thin disc perpendicular to the rotation axis for arbitrary Taylor numbers. Their results also suggest equations for the force-velocity relation for the steady translation of a rigid sphere for arbitrary Taylor numbers:

$$\frac{\mathbf{F}^H}{6\pi\mu a} = -\begin{bmatrix} 1+\frac{5}{7}\mathcal{T}^{1/2}+\frac{16\pi}{9(16+\pi^2)}\mathcal{T} & -\frac{3}{5}\mathcal{T}^{1/2}-\frac{4\pi^2}{9(16+\pi^2)}\mathcal{T} & 0 \\ \frac{3}{5}\mathcal{T}^{1/2}+\frac{4\pi^2}{9(16+\pi^2)}\mathcal{T} & 1+\frac{5}{7}\mathcal{T}^{1/2}+\frac{16\pi}{9(16+\pi^2)}\mathcal{T} & 0 \\ 0 & 0 & 1+\frac{4}{7}\mathcal{T}^{1/2}+\frac{8}{9\pi}\mathcal{T} \end{bmatrix} \cdot \mathbf{U}. \qquad (4.1)$$

This formula combines the low and high Taylor number results of, respectively, Herron et al. [31] and Stewartson [23].

5. Suspensions

Despite the variety of applications of centrifugal separation, there remain a number of unanswered questions concerning the rheological properties of multiphase mixtures undergoing rapid rotation. In particular, the appropriate form of the equations needed to adequately model such flows at arbitrary $\mathcal{T}$ has yet to be developed. Rotating mixtures have been considered from the approximate standpoint of two-phase flow theory [63], which has recently been applied in describing an experimental and numerical study of spin-up from rest of a mixture [64]. The topic of multiphase flow modeling of mixtures is described in a recent monograph by Ungarish [13]. In general, developing model two-phase flow equations for the motion of a mixture requires an assumption about the relative velocity between the particles and the fluid. Typically Stokes drag is used to deduce the particle velocities, even when it is inappropriate [13]. Recent research on the axial and transverse motion of isolated rigid particles has suggested simple expressions for the drag valid for *all* $\mathcal{T}$ (see equation 4.1) and so may prove valuable in modelling rotating suspensions.

The proper characterization of hydrodynamic interactions is necessary in order to calculate an effective stress tensor for a suspension. All models of multiphase rotating suspensions are limited by the lack of detailed knowledge concerning the hydrodynamic interactions between pairs of particles in rotating fluids. In particular, it is unknown to what extent the interaction of Taylor columns attached to individual particles influences the hydrodynamic forces resisting particle motion. For large particle Taylor numbers, for which Taylor columns with length $0.1a\mathcal{T}$ are expected (at least for axial translation, see Section 3.1), it is likely that some Taylor column interference occurs on the scale of individual particles when the volume fraction of suspended particles ϕ is larger than approximately $O(0.1\mathcal{T})^{-\frac{1}{3}}$ [13].

A more general approach for characterizing rotating mixtures would incorporate an exact representation of the flow on the scale of the microstructure. This method would combine the integral equation approach of Tanzosh & Stone [42], outlined in Section 3.4, with either Stokesian dynamics ideas [65] or low Reynolds number multi-particle simulations [66] in order to enable a computer simulation of rotating suspension flows valid for arbitrary Taylor numbers. An assessment of the computational feasibility of such an approach must await future research.

6. Analogous Flows

A number of recent developments described herein may be extended to particle motion problems in which entirely different physics gives rise to similar two-dimensional constraints on the motion of the suspending fluid. In this section, we indicate the analogies between particle motion in rotating fluids, stably stratified fluids and electrically conducting fluids permeated by a strong magnetic field, and refer the reader to more thorough treatments of the hydromagnetic and stratified flow problems.

6.1 Magnetohydrodynamics

The time evolution of the magnetic field $\mathbf{B}$ in an incompressible conducting fluid with magnetic diffusivity η is governed by the magnetic induction equation (e.g. [67]):

$$\frac{\partial \mathbf{B}}{\partial t} = \mathbf{B}\cdot\nabla\mathbf{u} - \mathbf{u}\cdot\nabla\mathbf{B} + \eta\,\nabla^2\mathbf{B}\,. \qquad (6.1)$$

If a quiescent fluid permeated by a strong uniform

magnetic field $\mathbf{B}_0$ is perturbed, then equation (6.1) indicates that any steady weak motions in a low magnetic diffusivity fluid must be two-dimensional (e.g. [68]):

$$\mathbf{B}_0 \cdot \nabla \mathbf{u} = 0 . \qquad (6.2)$$

Magnetic field thus acts in a manner analogous to a basic state vorticity field in a rotating system in suppressing velocity variations in the direction parallel to the field. As in a rapidly rotating fluid, slow steady particle motion is thus accompanied by a columnar region of blocked fluid. Detailed studies of particle motion in the presence of strong magnetic fields may be found in [69-72].

6.2 Stratified Fluids

The analogy between rapidly rotating and stably stratified fluids has been drawn in detail by Yih [73], Chandrasekhar [68] and Veronis [74]. For an incompressible stably stratified fluid in a vertical gravitational field, the continuity equation yields

$$\mathbf{u} \cdot \nabla \rho = 0 \qquad (6.3)$$

for steady flow of small amplitude. Vertical fluid motions are thus suppressed by the stratification, as work is required to drive such motions against gravity. Consequently, when a particle is dragged slowly in a horizontal direction through a stratified fluid, it will be accompanied by a horizontal column of fluid which is analogous to the Taylor columns observed in rotating fluids. Detailed studies of particle motion in stratified fluids and stratified 'Taylor columns' may be found in [75-77].

7. Conclusions

A broad overview of historical and recent studies of particle motion in rotating fluids has been presented. When viscous and inertial effects are sufficiently weak in the surrounding fluid, particle motion is accompanied by a Taylor column. The establishment of this dramatic blocked flow structure is generally accompanied by a drastic change in the hydrodynamic force on the particle.

The criteria for Taylor column formation are quite well defined in the axial problem; in particular, one expects a substantial Taylor column to develop in the high $\mathcal{T}$ limit provided $\mathcal{R}_o < 0.7$, otherwise the Taylor-Proudman constraint of two-dimensionality is relaxed by convective inertial effects. In the low $\mathcal{R}_o$ limit, the unbounded Taylor column has a characteristic length of $a\mathcal{T}/10$, which may be subdivided into a number of distinct flow regimes. In both the bounded and unbounded flow problems, the hydrodynamic force on a particle rising axially in the high $\mathcal{T}$ and low $\mathcal{R}_o$ limit is associated with geostrophic high and low pressure regions existing in, respectively, the up- and downstream Taylor column regions. In the unbounded problem, the rise speed depends only on the buoyancy and equatorial radius of the particle; consequently, a rigid disc, a rigid sphere and a fluid drop will all rise at the same rate provided they have identical equatorial radii and buoyancy forces. Conversely, in the bounded geometry, the axial rise speed depends further on the efficiency of the Ekman transport over the particle surface, and so on the shape of a rigid particle, or on the shape and fluid properties of a drop. Finally, the experimental confirmation of the theoretical predictions for the low $\mathcal{R}_o$ and high $\mathcal{T}$ limit is generally difficult owing to the persistence of inertial effects in the laboratory flows.

The criteria for Taylor column formation for transverse particle motion is more poorly understood. In the bounded geometry, the Hide criterion indicates when a Taylor column accompanying a fat body in the high $\mathcal{T}$ limit will span the entire fluid depth, and when it will be unstable to convective inertial influences. Specifically, it provides a critical $\mathcal{R}_o$ below which the flow around the body changes from three- to two-dimensional so that the hydrodynamic lift force becomes equal in magnitude to the Coriolis force which would act on the mass of fluid displaced by the particle. In the case of a neutrally buoyant sphere translating traversely with an accompanying Taylor column, the Coriolis and lift forces precisely cancel, and the drag on the body is comparable in magnitude to that associated with viscous effects. The precise magnitude of this viscous drag force is uncertain; in particular, it is unclear whether it corresponds to that on a spherical or columnar structure. In the low $\mathcal{R}_o$ limit, it is unclear when Taylor columns develop, and what their vertical extent might be. The development of an analogue of the Hide criterion for transverse particle motion at low

$\mathcal{R}_o$ remains an outstanding problem for theorists and experimentalists alike.

While the original studies of particle motion in rotating fluids were motivated by purely academic interest, there has been resurgent interest in such problems owing to their relevance in a variety of applications in industrial centrifugation processes. Through characterizing particle interactions in rotating suspensions, it is hoped that it will be possible to describe the bulk properties of such flows. Finally, it is hoped that a number of the mathematical and numerical techniques considered in this review may find wider application in related studies of particle motion in stratified fluids and particle motion in the presence of strong magnetic fields.

Acknowledgments

We thank the National Science Foundation for their support of this work through a PYI Award (CTS-8957043) to HAS. JWMB acknowledges a Postdoctoral Research Fellowship from the Natural Science and Engineering Research Council of Canada. We also thank Professor H. E. Emmons and Dr. J. D. Sherwood for several helpful conversations.
Figures 5, 9 and 12 and Table 1 were reprinted with the permission of Cambridge University Press.

References

1. Proudman, J. 1916. *Proc. Roy. Soc. A* **92**, 408–424.
2. Taylor, G.I. 1917. *Proc. R. Soc. A* **93**, 99–113.
3. Taylor, G.I. 1921. *Proc. R. Soc. A* **100**, 114–121.
4. Taylor, G.I. 1922. *Proc. Roy. Soc. Lond. A* **102**, 180–189.
5. Taylor, G.I. 1923. *Proc. Roy. Soc. A* **104**, 213–218.
6. Roberts, G.O., Kornfeld, D.M. & Fowlis, W.W. 1991. *J. Fluid Mech.* **229**, 555–567.
7. Annamalai, P., Subramanian, R.S. & Cole, R. 1982. *Phys. Fluids*, **25**, 1121–1126.
8. Bowen, T.J. 1970, *An Introduction to Ultracentrifugation*, Interscience, New York.
9. Annamalai, P., Shankar, N., Cole, R. & Subramanian, R.S. 1982. *Appl. Sci. Res.* **38**, 179–186.
10. Sherwood, J.D. 1986. *J. Fluid Mech.* **162**, 129–137.
11. Ambler, C.M. & Keith, F.W. 1978, In: E. S. Perry & A. Weissberger (editors) *Separation and Purification*, **12**, 295–347.
12. Hsu, H.-W. 1981, *Separations By Centrifugal Phenomena*, John Wiley.
13. Ungarish, M. 1993, *Hydrodynamics of Suspensions*, Springer-Verlag, Berlin.
14. Gould, W.J., Hendry, R. & Huppert, H.E. 1981. *Deep Sea Research* **28**, 409-440.
15. Baines, P.G. & Davies, P.A. 1980, In: *Orographic Effects in Planetary Flows*, GARP Publication Series, Geneva, 233-299.
16. Hide, R. 1961. *Nature* **190**, 213–218.
17. Stone, P.H. & Baker, D.J. 1968. *Quart. J. Roy. Met. Soc.* **94**, 576-580.
18. Marcus, P.H. 1988. *Nature* **331**, 693-696.
19. Moffatt, H.K. 1989. *Proc. IUTAM Symposium on Liquid Metal Magnetohydrodynamics*, Kluwer Academic Publications, 403–412.
20. Greenspan, H.P. 1968, *The Theory of Rotating Fluids*, Cambridge University Press.
21. Grace, S.F. 1926. *Proc. R. Soc. A* **113**, 46–77.
22. Stewartson, K. 1952. *Proc. Camb. Phil. Soc.* **48**, 168–177.
23. Stewartson, K. 1953. *Quart. J. Mech. Appl. Math.* **6**, 141–162.
24. Stewartson, K. 1958. *Quart. J. Mech. Appl. Math.* **11**, 39–51.
25. Stewartson, K. 1967. *J. Fluid Mech.* **30**, 357–369.
26. Moore, D.W. & Saffman, P.G. 1969. *J. Fluid Mech.* **39**, 831–847.
27. Annamalai, P. & Cole, R. 1986. *Phys. Fluids* **29**, 647–649.
28. Brone, D. & Cole, R. 1991. *Adv. Space Res.* **87**,

243–246.

29. Moll, H.G. 1973. *Ingenieur-Archiv.* **42**, 215–244.
30. Childress, S. 1964. *J. Fluid Mech.* **20**, 305–314.
31. Herron, I.H., Davis, S.H. & Bretherton, F.P. 1975. *J. Fluid Mech.* **68**, 209–234.
32. Batchelor, G.K. 1967, *An Introduction to Fluid Dynamics*, Cambridge University Press.
33. Berman, A.S., Bradford, J. & Lundgren, T.S. 1978. *J. Fluid Mech.* **84**, 411–431.
34. Baker, G.R. & Israeli, M. 1981. *Studies in Appl. Math.* **65**, 249–268.
35. Bush, J.W.M., Stone, H.A. & Bloxham, J. 1994. *J. Fluid Mech.* in press.
36. Long, R.R. 1953. *J. Met.* **10**, 197–203.
37. Stewartson, K. 1968. *Quart. J. Mech. Appl. Math.* **21**, 353–373.
38. Lighthill, M. J. 1967. *J. Fluid Mech.* **27**, 725–752.
39. Pritchard, W.G. 1969. *J. Fluid Mech.* **39**, 443–464.
40. Moore, D.W. & Saffman, P.G. 1969. *Phil. Trans. R. Soc. Lond. A* **264**, 597–634.
41. Maxworthy, T. 1970. *J. Fluid Mech.* **31**, 543–656.
42. Tanzosh, J.P. & Stone, H.A. 1994. *J. Fluid Mech.* **275**, 225–256.
43. Vedensky, D. & Ungarish, M. 1994. *J. Fluid Mech.* **262**, 1–26.
44. Morrison, J.W. & Morgan, G.W. 1956. Report 56207/8, Div. of Appl. Math. Brown University.
45. Weisenborn, A.J. 1985. *J. Fluid Mech.* **153**, 215–227.
46. Vonnegut, B. 1942. *Rev. Sci. Instr.* **13**, 6–9.
47. Rosenthal, D.K. 1962. *J. Fluid Mech.* **12**, 358–366.
48. Bush, J.W.M., Stone, H.A. & Bloxham, J. 1992. *Phys. Fluids* **4**, 1142–1147.
49. Moore, D.W. & Saffman, P.G. 1968. *J. Fluid Mech.* **31**, 635–642.
50. Hocking, L.M., Moore, D.W. & Walton, I.C. 1979. *J. Fluid Mech.* **90**, 781–793.
51. Ungarish, M. & Vedensky, D. 1994. *J. Fluid Mech.* to appear.
52. Stewartson, K. 1957. *J. Fluid Mech.* **3**, 17-26.
53. Maxworthy, T. 1965. *J. Fluid Mech.* **23**, 373-384.
54. Maxworthy, T. 1968. *J. Fluid Mech.* **31**, 643–653.
55. Hide, R. & Ibbetson, A. 1966. *Icarus* **5**, 279–290.
56. Hide, R., Ibbetson, A., & Lighthill, M.J. 1966. *J. Fluid Mech.* **32**, 251–272.
57. Tanzosh, J.P. & Stone, H.A. 1994. *J. Fluid Mech.* submitted.
58. Mason, P.J. 1975. *J. Fluid Mech.* **71**, 577–599.
59. Jacobs, S.J. 1964. *J. Fluid Mech.* **20**, 581–591.
60. Karanfilian, S.K. & Kotas, T.J. 1981. *Proc. R. Soc. Lond. A* **376**, 525–544.
61. Maxworthy, T. 1969. An Appendix to Moore & Saffman, *J. Fluid Mech.* **39**, 831–847.
62. Wilcox, D.C. 1972. *J. Fluid Mech.* **56**, 221–240.
63. Greenspan, H. P. & Ungarish, M. 1985. *J. Fluid Mech.* **157**, 359–373.
64. Amberg, G. & Ungarish, M. 1993. *J. Fluid Mech.* **246**, 443–464.
65. Brady, J.F. & Bossis, G. 1988. *Ann. Rev. Fluid Mech.* **20**, 111–157.
66. Kim, S. & Karrila, S.J. 1991, *Microhydrodynamics: Principles and Selected Applications*, Butterworth-Heinemann.
67. Shercliff, J.A. 1965, *A Textbook of Magnetohydrodynamics*, Pergamon Press, London.
68. Chandrasekhar, S. 1961, *Hydrodynamic and Hydromagnetic Stability*, Dover Publications, New York.
69. Chester, W. 1957. *J. Fluid Mech.* **3**, 304-308.
70. Chester, W. 1961. *J. Fluid Mech.* **10**, 459-465.
71. Maxworthy, T. 1968. *J. Fluid Mech.* **31**, 801-

814.

72. Kyrlidis, A., Brown, R. A. & Walker, J. S. 1990. *Phys. Fluids* **2**, 2230-2239.

73. Yih, C.-S. 1965, *Dynamics of Nonhomogeneous Fluids*, Macmillan, New York.

74. Veronis, G. 1970. *Ann. Rev. Fluid Mech.* **2**, 37-66.

75. Lin, Q., Lindberg, W. R., Boyer, D. L. & Fernando, H. J. S. 1992. *J. Fluid Mech.* **240**, 315-354.

76. Hanazaki, H. 1988. *J. Fluid Mech.* **192**, 393-419.

77. Foster, M. R. & Saffman, P. G. 1970. *J. Fluid Mech.* **43**, 407-418.